PROCEEDINGS OF THE ROYAL SOCIETY A MATHEMATICAL, PHYSICAL & ENGINEERING SCIENCES

Effects of microstructures on mesoscopic morphological transitions in deposition growth models

Pedro A. Sánchez, Tomás Sintes, Oreste Piro and Julyan H. E. Cartwright

Proc. R. Soc. A 2009 **465**, 3875-3884 first published online 7 October 2009
doi: 10.1098/rspa.2009.0311

PROCEEDINGS OF THE ROYAL SOCIETY A

Proc. R. Soc. A (2009) **465**, 3875–3884
doi:10.1098/rspa.2009.0311
Published online 7 October 2009

Effects of microstructures on mesoscopic morphological transitions in deposition growth models

By Pedro A. Sánchez[1,*], Tomás Sintes[1], Oreste Piro[1] and Julyan H. E. Cartwright[2]

[1]*Departamento de Física e Instituto de Física Interdisciplinar y Sistemas Complejos (Consejo Superior de Investigaciones Científicas – Universitat de les Illes Balears), Campus UIB, E-07122 Palma de Mallorca, Spain*
[2]*Instituto Andaluz de Ciencias de la Tierra (Consejo Superior de Investigaciones Científicas – Universidad de Grenada), Campus Fuentenueva, E-18002 Granada, Spain*

We study the influence of competing microstructure symmetries on the emergence of different morphologies during the growth by vapour deposition of thin solid films. We perform extensive numerical simulations with a minimal model that includes different microstructures, as well as thermal surface diffusion, to compute the corresponding structure zone model (SZM) and analyse, with statistical physics techniques, the details of transitional morphologies at border zones. We show that the maximum coordination number of the underlying microstructure provides a classification of the statistics of the transitional morphologies at the border between zones I (porous structures) and II (columnar faceted structures) of the SZM.

Keywords: non-equilibrium growth; physical vapour deposition; mesoscopic morphologies; structure zone model

1. Introduction

For many years, films of many different solid materials, both crystalline and amorphous, have been deposited from the vapour phase onto substrates with a great variety of deposition techniques. The field is driven by a huge number of technological applications to electronics, optics, chemistry and biology (Ohring 2001; Lakhtakia & Messier 2005), but also has much fundamental scientific interest, as understanding the basic physics involves taking up intriguing theoretical challenges imposed by non-equilibrium growth processes and interface physics; in particular, surface kinetic roughening of growing films has received much attention as a dynamical system that exhibits non-equilibrium critical behaviour (Barabási & Stanley 1995; Meakin 1997; Ódor 2004; Katzav *et al.* 2006; Silveira & Aarão Reis 2007).

*Author for correspondence (pedro@ifisc.uib-csic.es).

Received 11 June 2009
Accepted 7 September 2009

One of the key differences between films and bulk solids is in their mesoscale morphologies. The study of solid film morphology has a long history, and, from the 1960s onwards, efforts have been made to construct a classification of the morphology of a film depending on its deposition conditions. This has culminated in the empirical structure zone model (SZM), which describes well the universal trends seen in experiments with many different materials. The model has been progressively revised and updated, and there are now recognized to be at least five distinct zones with differing mesoscale morphologies (Lakhtakia & Messier 2005). From the modelling point of view, several strategies have been proposed to describe qualitatively the essential features of the SZM, among which ballistic deposition models are prominent. However, in spite of this great progress, little effort has been devoted to characterization of transitional structures at parameters near the border zones. In particular, the impact of the symmetries of the microstructure on the nature of these transitional structures has not been analysed deeply, either experimentally or theoretically.

The main purpose of this paper is to go beyond the qualitative description of the similarities observed within each structure zone and investigate, by means of simulations, the influence of the material microstructure symmetries on the transitional mesoscale morphologies of the grown film. To this end, we have developed a minimal model of the physics of solid film growth operating at the interface between the molecular scale and the mesoscale. Our simulations show that the statistical features of the transitional film morphologies obtained when going from the so-called zone I in the SZM (characterized by the formation of fractal-like patterns) to the zone II (where pronounced faceting emerges with the ulterior formation of characteristic smooth surfaces) depend on the maximum coordination number of the underlying microstructure. We also show that distinct microstructures have clearly discernable effects on the evolution of the characteristic sizes of compact mesoscopic structures that compose the films in zone II. These results demonstrate the relevance of the incorporation of realistic microstructures to mesoscopic film growth simulations.

2. The model

One of the main difficulties in the study of thin film growth is the wide range of length and time scales involved. Molecular dynamics simulation is an appropriate technique because of its ability to model the dynamics at a microscopic level, but it has the inherent disadvantage that time steps shorter than 10^{-13} s are needed to correctly incorporate the atomic vibrations. More efficient algorithms of this kind were recently developed using the concept of a thermal control layer (Lin *et al.* 2005). However, a very successful and frequently used alternative is to exclude the details of the atomic vibrations and to concentrate on the atomic mobility processes simulating them as stochastic events with Monte Carlo methods. We follow the latter approach using kinetic Monte Carlo simulations of the superficial diffusion in combination with a ballistic algorithm adapted to include different microstructure symmetries to model the deposition process.

More specifically, in our model, the depositing units (atoms, molecules or clusters, sometime called growth units or adatoms) are represented as hard discs of radius a located by the positions of their centres. These discs are ballistically deposited on a one-dimensional substrate with periodic boundary conditions at a mean rate R. The ballistic trajectories are taken to be normal to the substrate, which is initially configured as a monolayer of fixed adatoms in a close-packed arrangement. Bonds between adatoms are restricted to nearest neighbours. On making the first contact, either with the adatoms on the film surface or directly with the substrate, the incoming particles are instantaneously relocated at the closest available attachment site defined in the considered microstructure. For the microstructures, we generalize the off-lattice scheme of Savaloni & Shahraki (2004) where, instead of fixed lattice positions, there is a set of relative positions, the so-called *active positions*, around each particle of the film, which are possible locations of any bonded neighbours. In other words, bonding sites for first nearest neighbours are not fixed with respect to the substrate but localized around the exposed adatoms. Savaloni & Shahraki (2004) introduced this approach to study the complex microstructure formed by the superposition of the elementary bidimensional cells corresponding to simple square and hexagonal lattices. However, the same approach can be used for either simple or complex microstructures. We have studied the four different microstructure combinations shown schematically in figure 1: the purely square (sq) and the purely hexagonal (hex) lattices, the hexagonal–square (hex–sq) microstructure—formed by the superposition of the previous ones—and the square–square microstructure (sq–sq) obtained by the superposition of two purely square latices, one horizontal as the substrate and the other one tilted 45°. The available sites to accomodate the incoming particles from their first contact position with the film surface are the empty and non-shadowed active positions of the surrounding surface adatoms. After a new surface adatom is accommodated, bonds with its nearest neighbours are established and the corresponding new unoccupied active positions are created around it. Simultaneously with the deposition of new particles, surface adatoms are allowed to diffuse thermally to any of the close active positions that are neither occupied nor shadowed. Adatoms are considered as belonging to the surface when they are not 'buried' by the presence of neighbours in the top active positions. In our simulations, diffusive hops to active positions are restricted to a neighbourhood of size $2a$ around the original adatom position, except for the square microstructure where the small number of available active positions makes the compactification of the mesoscopic structures difficult if hops to second-nearest neighbours are not allowed. We thus allow 'over-a-step' hops for the purely square (sq) microstructure.

In order to simulate the surface diffusion during the film growth, we apply, as we anticipated, the kinetic Monte Carlo method (Levi & Kotrla 1997). This method evaluates the transition probabilities between states of a system governed by a set of stochastic events with a given mean rate. In our case, the events are composed of the deposition of a new particle with a constant mean rate R, and all the possible diffusive hops of the surface particles, whose mean rates themselves depend on the surface configuration. We use the same estimates used by Müller (1985) and Savaloni & Shahraki (2004) for the mean rates of surface-diffusion hops. Assuming that diffusive hops are activated by thermal fluctuations with frequency $\nu = 2kT/h$, the characteristic mean rate for each possible hop can be

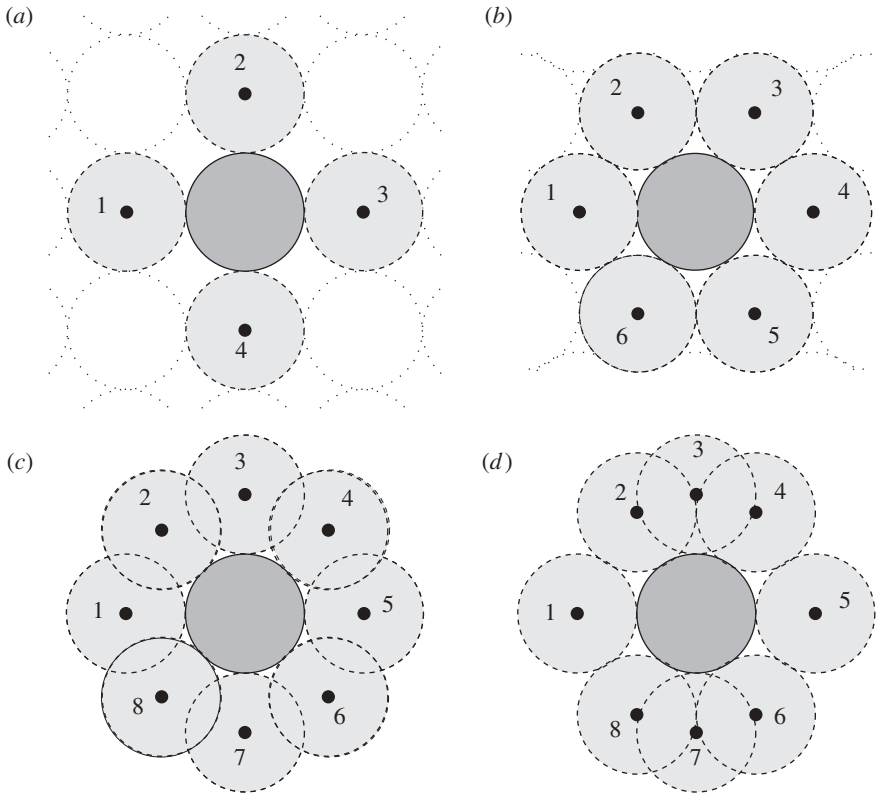

Figure 1. Microstructures used in our simulations with their active positions labelled. (*a*) Simple square lattice with a maximum coordination number 4; a particle is buried when active position 2 is occupied. (*b*) Simple hexagonal lattice with a maximum coordination number 6; a particle is buried when active positions 2 and 3 are occupied. (*c*) Double square lattice with a maximum coordination number 4; a particle is buried when active positions 2, 3 and 4 are occupied. (*d*) Two-dimensional projection of the face-centered cubic lattice (square and hexagonal lattices mixed); the maximum coordination number is 6; a particle is buried when active positions 2, 3 and 4 are occupied.

computed from Boltzmann statistics, and we obtain

$$R_{i\to j} = \nu \exp\left(-\frac{\Delta E_{i\to j}}{kT}\right), \tag{2.1}$$

where $\Delta E_{i\to j}$ is the activation energy barrier for the hop between positions i and j. Müller (1985) estimated these barrier heights in terms of the number of bonded neighbours at the origin and destination positions (respectively, N_i and N_j) as

$$\Delta E_{i\to j} = \begin{cases} Q, & N_i \le N_j, \\ Q + (N_j - N_i)\phi, & N_i > N_j, \end{cases} \tag{2.2}$$

where ϕ is the bonding potential and Q is the surface-diffusion activation energy, which is given as a function of the substrate temperature T and the melting point

of the material T_m by the empirical expression of Neumann & Hirchswald (1972),

$$Q = \left(5 + \frac{20}{3}\frac{T}{T_m}\right) kT_m \quad (T < 0.5\ T_m). \tag{2.3}$$

At each simulation step, we compose the list of the rates for the M possible dynamical events of the system—the mean rates of the $M-1$ possible diffusion hops given by equation (2.1) and the mean deposition rate R. Then, one event m is randomly selected from the list, with a probability given by its relative mean rate, through the condition

$$\frac{\sum_{i=0}^{m-1} R_i}{\sum_{i=1}^{M} R_i} < r < \frac{\sum_{i=1}^{m} R_i}{\sum_{i=1}^{M} R_i} \quad (R_0 = 0), \tag{2.4}$$

where r is a flat random number drawn from the interval $(0, 1)$. After the event is completed, the events list is updated according to the new configuration of the system and the dynamical time step is increased by

$$\delta t = -\ln(r') \left[\sum_{i=1}^{M} R_i\right]^{-1}, \tag{2.5}$$

where r' is another flat random number from the interval (0, 1). In our simulations, we deposited 15 000 particles onto a flat substrate prepared by disposing 160 adatoms in a close-packed arrangement. For the type of interactions considered here, this system size is large enough to preclude important finite size effects. For the sake of comparison with the previous results from the work of Savaloni & Shahraki (2004), we picked the same physical parameters corresponding to nickel: $T_m = 1720\,\mathrm{K}$, $\phi = -0.74\,\mathrm{eV}$ and $a = 0.352\,\mathrm{nm}$.

3. Results

As the substrate temperature—one of the two most important deposition parameters—is varied, one observes the development of different characteristic mesoscopic film morphologies. In figure 2, we show the sequences of film morphologies that emerged for each microscopic symmetry combination considered at the same sequence of different substrate temperatures and a fixed deposition rate R of one monolayer per second ($\mathrm{ML\,s^{-1}}$). In all cases, we found a minimum substrate temperature below which low-density dendritic structures are obtained. These structures are characterized by a self-affine surface typically observed in ballistic deposition models that neglect surface diffusion. As the substrate temperature increases, or equivalently as deposition rate decreases, surface diffusion becomes significant, and dendritic morphologies give rise to more compact fibrous structures with a preferential growth axis parallel to the deposition trajectories. With even greater surface diffusion, the former fibrous structures become compact, giving rise to densely packed grains that grow vertically as competing columns whose thickness increases with the diffusion. This behaviour, qualitatively independent of the underlying microstructure, characterizes the transition, in the context

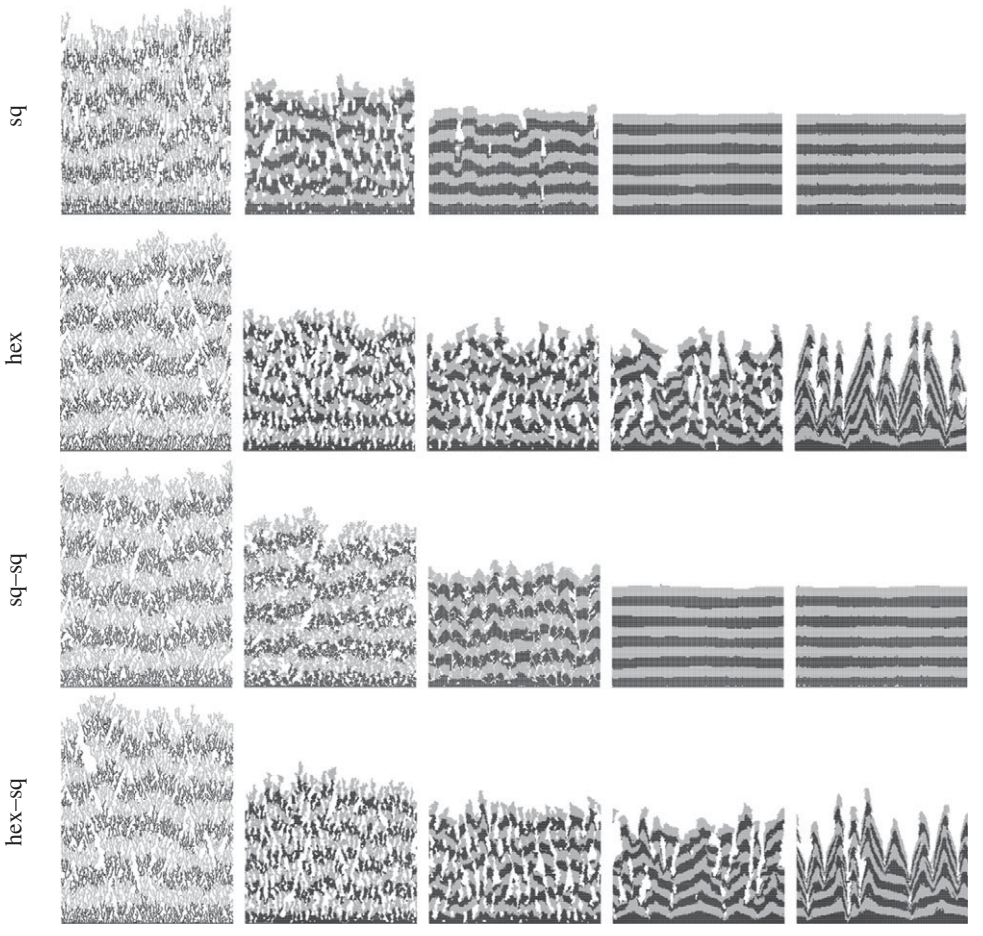

Figure 2. Film structures obtained at different temperatures at a fixed deposition rate of $1\,\mathrm{ML\,s^{-1}}$ for each given microstructure; to aid the eye, each stripe represents a height of 10 ML. $T/T_\mathrm{m} = 0.12$, 0.23, 0.26, 0.40 and 0.47.

of the SZM (Movchan & Demchishin 1969; Lakhtakia & Messier 2005), from the typical morphologies found in zone I, which is fractal-like, to zones IIa, where pronounced faceting develops, and IIb, characterized by smooth surfaces. We should emphasize here that, as our model does not include any other significant parameters to describe grain boundary evolutions than the underlying microstructure and the competition between deposition rates and surface diffusion, it is not suitable for the investigation of other zones of the SZM where effects such as activated diffusion by ion bombardment of the surface, bulk diffusion or the presence of impurities are believed to be determinant (Lakhtakia & Messier 2005).

For those microstructures with a maximum coordination number of 4 such as the simple square sq and the square–square sq–sq, we found that, as surface diffusion increases, the thickness of the column eventually reaches the system size. As a consequence, the films form a single compact structure without interstitial voids. Interestingly, however, this is not the case, at least in the range of

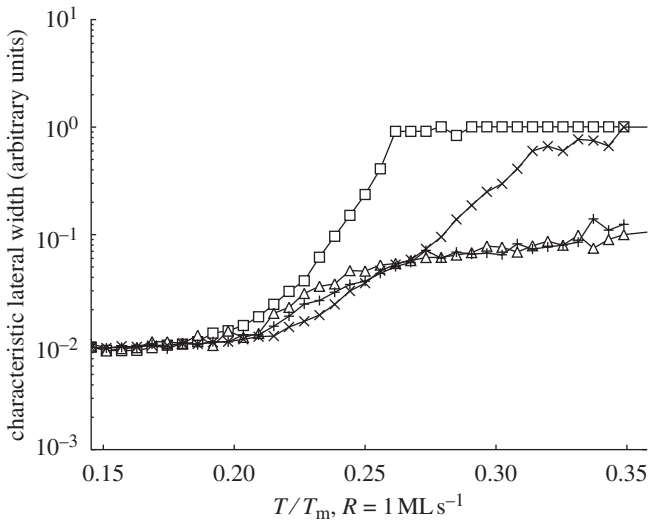

Figure 3. Change of the mean column width of dense structures with substrate temperature. Values are plotted relative to the total width of the substrate. Line with open square, sq; line with open triangle, hex; line with cross, sq–sq; line with plus, hex–sq.

temperatures studied, for the hex and hex–sq microstructures, which have a maximum coordination number of 6. As a consequence, in spite of their qualitative universal character, the sequence of emergent mesoscopic morphologies as the deposition parameters are varied seems to be significantly influenced by the underlying microstructure, as shown in figure 2. The increase of the dense column width and the concomitant reduction of intercolumnar voids is substantially faster in the case of microstructures with a smaller maximum coordination number. This is an intuitive consequence of the diffusion because compact particle arrangements with higher maxima of the coordination number tend to form frozen structures more easily, making lateral grain boundary diffusion more difficult. This effect can be further illustrated by the measure of the average lateral width of dense structures, shown in figure 3. This magnitude has been sampled by averaging the horizontal lengths at the central regions of the films of zones with a local mean packing density above 0.75, the maximum density allowed by the microstucture. At high temperatures, the characteristic widths for hex and hex–sq microstructures are very similar and lower than those observed for the sq and sq–sq microstructures. It is also notable how the simple square microstructure benefits from diffusion hops to second-nearest neighbours to reduce the interstitial voids and increase the characteristic columnar width.

The mean packing density is a property frequently used to characterize the film morphology (Müller 1985; Brett 1989; Savaloni & Shahraki 2004). In simple atomistic simulations, the value of the mean packing density increases with surface diffusion following a sigmoidal law. The sigmoid curves obtained for the mean packing density, or for other statistical magnitudes that characterize the particle arrangements in the film, are commonly used to establish the limits between different structure zones, but the way in which these limits are estimated differs. Müller (1985) defined a characteristic temperature that fixes the limit

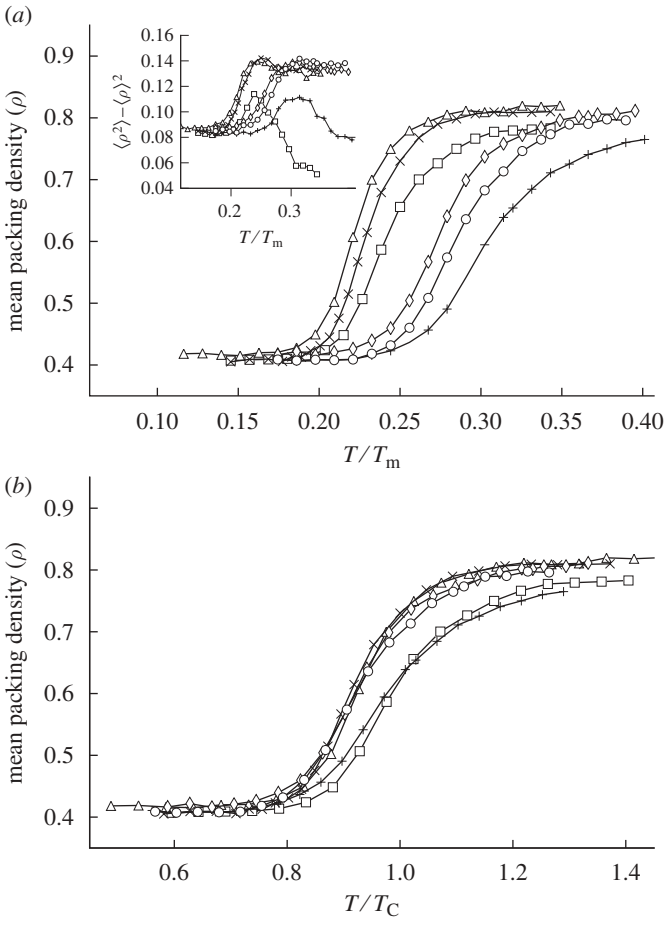

Figure 4. (*a*) Change of the bulk mean packing density ρ with the substrate temperature T, obtained for different microstructures and at deposition rates $R = 1$ and $100\,\mathrm{ML\,s^{-1}}$. The location of the maxima of their statistical fluctuations (inset figure) determines the characteristic temperature of each curve, T_C. (*b*) Mean packing density curves rescaled with the characteristic transition temperature T_C. Curves corresponding to the microstructures sharing the same maximum coordination number collapse onto a single master curve. Line with open square, $R = 1\,\mathrm{ML\,s^{-1}}$, sq–sq; line with open triangle, $R = 1\,\mathrm{ML\,s^{-1}}$, hex; line with cross, $R = 1\,\mathrm{ML\,s^{-1}}$, hex–sq; line with plus, $R = 100\,\mathrm{ML\,s^{-1}}$, sq–sq; line with open diamond, $R = 100\,\mathrm{ML\,s^{-1}}$, hex; line with open circle, $R = 100\,\mathrm{ML\,s^{-1}}$, hex–sq.

between structure zones I and II from the inflexion point of the curve. On the other hand, Savaloni & Shahraki (2004) claimed that zones I, II and III correspond to segments having different slopes in the same sigmoidal curve. As our model is restricted to structure zones I and II, we are closer to Müller's interpretation, but in order to establish a consistent criterion to characterize the structure zone limits, we perform a detailed examination of the statistical fluctuations along these transition curves.

In figure 4*a* we represent the change of the mean packing density ρ with the substrate temperature for three different microstructures at two different deposition rates $R = 1$ and $100\,\mathrm{ML\,s^{-1}}$. This has been calculated by sampling

the fraction of the occupied volume in small regions around adatoms over the whole film structure, excluding the substrate. The computed statistical fluctuations are shown in the inset plot of figure 4*a*. For all the microsctructures and deposition rates studied, we found a maximum in the statistical fluctuations of the mean packing density that can be used to identify a characteristic transition temperature from zone I to zone II in the SZM. After normalizing the mean packing density curves with their characteristic transition temperature, T_C, we observe that all the curves corresponding to microstructures sharing the same maximum coordination number collapse onto a single master curve. In fact, as the maximum coordination number for sq and sq–sq microstructures is 4 and for hex and hex–sq is 6, we find the two sets of curves shown in figure 4*b*. This result, in agreement with the typical morphologies of the film structures obtained (figure 2), and the change in the mean column width of the dense structures (figure 3), is a clear indication of the relevance of the underlying microstructure to the structural transitions in solid film growth. Moreover, the change in the structure at the mesoscopic level seems to be governed by the value of the maximum coordination number of the microstructure.

4. Conclusions

In summary, our work strongly suggests that microstructures at the molecular level might have important quantitative influences on the development of film morphologies. For all microstructures, the increase of surface diffusion and the consequent reduction of the shadowing effect, as the substrate temperature increases, give rise to structures that go from an extremely porous fractal-like pattern (corresponding to zone I in the SZM), to a well-defined columnar faceted structure with smooth surface (corresponding to zone II). However, the characteristic temperature at which the transition from zone I to zone II takes place clearly depends on the maximum coordination number of the microstructure. For example, as figure 2 suggests, higher values of the maximum coordination number lead more easily to frozen fractal structures, so that higher substrate temperatures are required to reach zone II. We find that the mean packing density as a function of the substrate temperature is an appropriate parameter to characterize the film morphology. Remarkably, this function is found to collapse onto different master curves when rescaled with respect to the characteristic transition temperature derived from the maximum of the density packing fluctuations. Moreover, these master curves are associated with microstructures sharing the same maximum coordination number. These results suggest that the mean coordination number is another appropriate parameter to characterize the structural transitions in solid film growth. However, we expect that this parameter will also amplify the epitaxial effects on the growth process. A detailed analysis of the behaviour of this parameter will be provided elsewhere (P. A. Sánchez, T. Sintes, J. H. E. Cartwright & O. Piro 2009, unpublished data). As a final remark, our simulations also suggest the possible existence of a simile of a non-equilibrium continuous phase transition in the development of different film morphologies, in analogy to what happens in many other non-equilibrium particle systems, such as the directed percolation model (Ódor 2004). There, a continuous transition from a frozen absorbed state to an active state is

observed in the evolution of the system produced by different values of the control parameter. Although a direct change from one phase to the other is not possible by changing such a parameter, the statistics of the resulting states shows the scaling properties of a phase transition. This analogy should stimulate future work on the characterization of such morphological phase transitions in the SZM model.

We thank Russ Messier for useful conversations. This work was undertaken with the financial support of the CSIC project Hielocris. T.S. also ackowledges project FIS2007-60327.

References

Barabási, A.-L. & Stanley, H. E. 1995 *Fractal concepts in surface growth*. Cambridge, UK: Cambridge University Press.

Brett, M. J. 1989 Simulation of structural transitions in thin films. *J. Mater. Sci.* **24**, 623–626. (doi:10.1007/BF01107452)

Katzav, E., Edwards, S. F. & Schwartz, M. 2006 Structure below the growing surface. *Europhys. Lett.* **75**, 29–35. (doi:10.1209/epl/i2006-10077-9)

Lakhtakia, A. & Messier, R. F. 2005 *Sculptured thin films: nanoengineered morphology and optics*. Bellingham, WA: SPIE Press.

Levi, A. C. & Kotrla, M. 1997 Theory and simulation of crystal growth. *J. Phys., Condens. Matter* **9**, 299–344. (doi:10.1088/0953-8984/9/2/001)

Lin, H.-C., Chang, J.-G., Ju, S.-P., & Hwang, C.-C. 2005 A general consideration of incident impact energy accumulation in molecular dynamics thin film simulations—a new approach using thermal control layer marching algorithms. *Proc. R. Soc. A* **461**, 3977–3998. (doi:10.1098/rspa.2005.1539)

Meakin, P. 1997 *Fractals, scaling and growth far from equilibrium*. Cambridge, UK: Cambridge University Press.

Movchan, B. A. & Demchishin, A. V. 1969 Study of structure and properties of thick vacuum condensates of nickel, titanium, tungsten, aluminium oxide and zirconium dioxide. *Phys. Met. Metallogr.* **28**, 83–88.

Müller, K.-H. 1985 Dependence of thin-film microstructure on deposition rate by means of a computer simulation. *J. Appl. Phys.* **58**, 2573–2576. (doi:10.1063/1.335885)

Neumann, G. & Hirchswald, W. 1972 Mechanisms of surface self-diffusion. *Z. Phys. Chem. B* **81**, 163–176.

Ódor, G. 2004 Universality classes in nonequilibrium lattice systems. *Rev. Mod. Phys.* **76**, 663–724. (doi:10.1103/RevModPhys.76.663)

Ohring, M. 2001 *The materials science of thin films*, 2nd edn. New York, NY: Academic Press.

Savaloni, H. & Shahraki, M. G. 2004 A computer model for the growth of thin films in a structure zone model. *Nanotechnology* **15**, 311–319. (doi:10.1088/0957-4484/15/3/014)

Silveira, F. A. & Aarão Reis, F. D. A. 2007 Surface and bulk properties of deposits grown with a bidisperse ballistic deposition model. *Phys. Rev. E* **75**, 061 608. (doi:10.1103/PhysRevE.75.061608)